

Diagnostic Performance of ^{124}I -Metaiodobenzylguanidine PET/CT in Patients with Pheochromocytoma

Manuel Weber^{1,2}, Jochen Schmitz^{1,2}, Ines Maric^{1,2}, Kim Pabst^{1,2}, Lale Umutlu^{2,3}, Martin Walz⁴, Ken Herrmann^{1,2}, Christoph Rischpler^{1,2}, Frank Weber^{2,5}, Walter Jentzen^{1,2}, Sarah Theurer^{2,6}, Thorsten D. Poeppel⁷, Nicole Unger^{*2,8}, and Wolfgang P. Fendler^{*1,2}

¹Department of Nuclear Medicine, University Hospital Essen, Essen, Germany; ²German Cancer Consortium, Essen, Germany;

³Department of Diagnostic and Interventional Radiology and Neuroradiology, University Hospital Essen, Essen, Germany;

⁴Department of Surgery and Center of Minimally Invasive Surgery, Evangelische Kliniken Essen–Mitte, Academic Teaching Hospital of University Duisburg–Essen, Essen, Germany; ⁵Department of General, Visceral, and Transplantation Surgery, Section of Endocrine Surgery, University of Duisburg–Essen, Essen, Germany; ⁶Institute of Pathology, University Hospital Essen, University Duisburg–Essen, Essen, Germany; ⁷Nuklearmedizin, MVZ CDT Strahleninstitut, Cologne, Germany; and ⁸Division of Laboratory Research, Department of Endocrinology and Metabolism, University Hospital Essen, University Duisburg–Essen, Essen, Germany

$^{123/131}\text{I}$ -metaiodobenzylguanidine (MIBG) scintigraphy has shown a high specificity for imaging pheochromocytoma and paraganglioma, but with low sensitivity because of low spatial resolution. ^{124}I -MIBG PET may be able to overcome this limitation and improve the staging of patients with (suspected) pheochromocytoma. **Methods:** We analyzed the sensitivity, specificity, and positive and negative predictive values of ^{124}I -MIBG PET in 43 consecutive patients with suspected (recurrence of) pheochromocytoma using histopathologic ($n = 25$) and clinical validation ($n = 18$) as the standard of truth. Furthermore, we compared the detection rate of ^{124}I -MIBG PET versus contrast-enhanced (CE) CT on a per-patient and per-lesion basis in 13 additional patients with known metastatic malignant pheochromocytoma. **Results:** ^{124}I -MIBG PET/CT was positive in 19 (44%) of 43 patients with suspected pheochromocytoma. The presence of pheochromocytoma was confirmed in 22 (51%) of 43. ^{124}I -MIBG PET/CT sensitivity, specificity, and positive and negative predictive values were 86%, 100%, 100%, and 88%, respectively. ^{124}I -MIBG PET was positive in 11 (85%) of 13 patients with malignant pheochromocytoma. Combined ^{124}I -MIBG PET and CE CT detected 173 lesions, of which 166 (96%) and 118 (68%) were visible on ^{124}I -MIBG PET and CE CT, respectively. **Conclusion:** ^{124}I -MIBG PET detects pheochromocytoma with high accuracy at initial staging and a high detection rate at restaging. Future assessment of ^{124}I -MIBG PET for treatment guidance, including personalized ^{131}I -MIBG therapy, is warranted.

Key Words: ^{124}I -MIBG PET; pheochromocytoma; theranostics

J Nucl Med 2022; 63:869–874

DOI: 10.2967/jnumed.121.262797

Metaiodobenzylguanidine (MIBG), or iobenguane, is an analog of the adrenergic neurotransmitter norepinephrine and shows uptake in sympathetically innervated tissues such as the heart and salivary glands and tumors that express norepinephrine

transporters (1). Because of high accumulation and retention in sympathicomodullary tissue, $^{123}\text{I}/^{131}\text{I}$ -MIBG scintigraphy has been used for decades in the imaging of pheochromocytoma and paraganglioma, as well as in many neural crest tumors, with reported sensitivities and specificities of between 80% and 100% (2–4). The sensitivity is hampered considerably by a low spatial resolution, making the assessment of small lesions particularly challenging (5). Because of superior technology and workflows, PET expanded rapidly (6) and is now the standard imaging modality for most cancer entities, including pretherapeutic imaging in patients with neuroendocrine tumors (7) and prostate cancer (8,9). In patients with pheochromocytoma and paraganglioma, somatostatin receptor–targeted PET (10–12) and ^{18}F -flubrobenguane (13) have shown a high specific uptake and a high sensitivity. However, ^{124}I -MIBG PET comes with several potential advantages.

The similarity in its biodistribution to that of ^{123}I -MIBG allows for the translation of current concepts for image interpretation (e.g., SIOPEN [International Society of Paediatric Oncology European Neuroblastoma] and curie), protocols, and medications established by use of ^{123}I -MIBG scintigraphy (14,15).

Furthermore, ^{124}I -MIBG PET potentially combines the high specificity of MIBG imaging with the high sensitivity (5,16) and better quantification of PET tracers (17–19) and thereby addresses major shortcomings of current γ -emitting compounds.

In addition, the long ^{124}I half-life (4.18 d) allows for the assessment of pharmacokinetics by performing imaging and blood tests at multiple time points (18,20–23). Following the theranostic principle, the sister compound ^{131}I -labeled MIBG is applied for radionuclide therapy. In light of the recent Food and Drug Administration approval of ^{131}I -MIBG (24) for the treatment of unresectable, locally advanced, and metastatic pheochromocytoma and paraganglioma, pretherapeutic ^{124}I -MIBG PET can provide valuable information on absorbed doses to the tumor and organs at risk and thereby lay the foundation for personalized dosimetry and activity escalation. The potential of the theranostic pair $^{124}\text{I}/^{131}\text{I}$ to improve efficacy and mitigate toxicity has previously been shown in the treatment of patients with differentiated thyroid cancer (20,21,23,25) and in a case report on $^{124}\text{I}/^{131}\text{I}$ -MIBG (18).

The aim of this retrospective study was to assess the diagnostic performance of ^{124}I -MIBG PET in patients with suspected pheochromocytoma and in patients with metastatic malignant

Received Jul. 6, 2021; revision accepted Sep. 8, 2021.

For correspondence and reprints, contact Manuel Weber (manuel.weber@uk-essen.de).

*Contributed equally to this work.

Published online Sep. 23, 2021.

COPYRIGHT © 2022 by the Society of Nuclear Medicine and Molecular Imaging.

pheochromocytoma (MMP) before ^{131}I -MIBG therapy. With this intent, we analyzed the optimal imaging time point with regard to tumor uptake, the accuracy in comparison to CT, and the rate of upstaging by use of ^{124}I -MIBG PET in patients with MMP.

MATERIALS AND METHODS

Study Design and Participants

We screened our institutional database for patients who, between March 2005 and March 2017, underwent ^{124}I -MIBG PET/CT for suspected recurrence of adrenal pheochromocytoma and who had sufficient follow-up data for validation. The primary endpoint in these patients was the diagnostic performance, defined as sensitivity, specificity, and negative and positive predictive value. Validation was performed histopathologically or—when histopathology was not available—by an experienced, board-certified endocrinologist on the basis of clinical and laboratory parameters. Secondary endpoints were the diagnostic power of quantitative assessment using SUV_{peak} for differentiating between patients for whom the suspected pheochromocytoma was confirmed versus those for whom it was ruled out. A subgroup analysis was performed for patients who met the criteria for an indeterminate adrenal mass (size > 10 mm and Hounsfield units [HU] > 10 on non-contrast-enhanced [NC] CT).

For a second analysis, we included patients with known metastatic MMP. The primary metric in this cohort was the lesion detection rate of ^{124}I -MIBG PET using the sum of all detected lesions in conjunction with coacquired contrast-enhanced (CE) CT as the reference standard. The protocol was approved by the Ethics Commission of the University of Duisburg-Essen medical faculty (protocol 20-9656-BO).

^{124}I -MIBG Synthesis

^{124}I -MIBG was manually prepared by the substitution of non-carrier-added ^{124}I -iodine to MIBG. The labeling was performed via copper(I)-assisted isotopic iodine/iodide exchange. ^{124}I -iodine was purchased from PerkinElmer LAS in the form of sodium iodide (^{124}I) as 0.02N NaOH solution. Glacial acetic acid (Merck KGaA) was used as the solvent for all other reactants. Typically, 100–130 MBq of the ^{124}I solution were transferred into a testing tube, 10 μL of a sodium disulfite solution (4 mg/mL) were added, and the mixture was reduced to dryness using a rotating evaporator. A 40- μL volume of a solution containing 100 μg of metaiodobenzylguanidine (Sigma-Aldrich) and 1.5 μL of $\text{Cu}(\text{I})\text{Cl}$ (0.1 M; Merck KGaA) was added to the residue. The mixture was then heated in the stoppered testing tube at 160°C for 10 min. After the subsequent reduction to dryness, the raw product was resolved in 80–100 μL of hydrochloric acid (0.01 M, aqueous; Sigma-Aldrich) and the volume was injected into a high-performance liquid chromatography system (Waters) for purification. The semipreparative high-performance liquid chromatography was performed isocratically using a LiChroCART 250-4 column (Purospher RP-18, 5 μm ; Merck) with radioactivity and ultraviolet detection (254 nm), the eluent being an aqueous solution of NaH_2PO_4 (1.38 g/L) and acetonitrile, 9:1 (v/v). The product peak (retention time, 13 min; activity channel) was collected in a round-bottom flask, and the volume was reduced to dryness and formulated in 5 mL of phosphate-buffered saline. The volume was collected into a syringe and passed through a 0.22- μm filter (Millex GV; Millipore) directly into a sterile vial (Cis-Bio), yielding 50–70 MBq of formulated ^{124}I -MIBG. Quality control testing of the product was performed using a high-performance liquid chromatography system identical to that for the semipreparative run. Purity was determined to be between 98% and 100%.

Imaging Protocol

PET/CT was performed on a Siemens Duo ($n = 40$, 71%), Siemens Biograph mCT ($n = 15$, 27%), or Siemens Biograph mMR ($n = 1$,

2%) at 4 h ($n = 26$), 1 d ($n = 53$), 2 d ($n = 33$), and 4 or 5 d ($n = 11$) after the administration of a mean activity of 49.8 (interquartile range, 48.3–53.0) MBq of ^{124}I -MIBG. The emission time was 3 min 30 s per bed position for PET/CT and 8 min for PET/MRI. Attenuation correction was performed with the coacquired CT or MRI scan.

Image Analysis

SUV_{peak} was measured in the 5 lesions displaying the highest tracer uptake for each MMP patient at all imaging time points, with the aim of identifying the imaging time point with the highest average SUV_{peak} and tumor-to-background ratio, with SUV_{mean} liver as the reference background.

The ^{124}I -MIBG PET/CT images of all preoperative or recurrent pheochromocytomas at this time point were then read by a masked central reader, and pathologic findings were categorized by anatomic region (adrenal gland, bones, or viscera, including distant lymph nodes). The size, SUV_{peak} , and HU of the adrenal masses on the NC CT images were measured. The CE CT and ^{124}I -MIBG PET/CT images were anonymized separately and read by a masked reader, with at least 2 wk elapsing between reading sessions to avoid recall bias.

Statistical Analysis

The accuracy of ^{124}I -MIBG PET is reported by descriptive statistics. For an indeterminate adrenal mass, separate analyses were performed using the NC CT criteria (>10 HU and >10 mm) versus combined ^{124}I -MIBG PET and NC CT criteria (^{124}I -MIBG PET-positive or adrenal mass >10 HU and >10 mm). The detection rate for patients with MMP was defined as the fraction of ^{124}I -MIBG PET-positive lesions among all lesions for CE CT and ^{124}I -MIBG PET/CT combined. Statistical analysis was performed using SPSS Statistics, version 26 (IBM Corp.). Mann-Whitney U testing was performed to determine the statistical significance of SUV_{peak} between patients with and without pheochromocytoma. A receiver-operating-characteristic curve, with area under the curve as a metric, was used to determine the predictive potential of SUV_{peak} for the diagnosis of pheochromocytoma, after the exclusion of 1 patient for whom images were acquired 2 d after the administration of ^{124}I -MIBG. The Youden J statistic was used to identify the optimal cutoff for the diagnosis of pheochromocytoma based on the SUV_{peak} for all patients and separately for patients with an indeterminate adrenal mass.

RESULTS

Patient Cohort

Fifty-six consecutive patients were eligible. In 43 of 56 patients ^{124}I -MIBG PET was performed for suspected pheochromocytoma because of an elevated catecholamine metabolite level, an unclear renal mass, or the clinical appearance; 4 of these were examined because of suspected recurrence after initial resection. Patient characteristics are given in Table 1. The mean patient age was 51.8 y (range, 20–74 y); 25 patients (58%) were female, and 18 (42%) were male. Three patients (7%) had multiple endocrine neoplasia type IIA, and one (2%) had neurofibromatosis type 1. The mean levels for metanephrine and normetanephrine were 180.9 pg/mL (range, 15–1,377 pg/mL) and 313.8 pg/mL (range, 28–2,358 pg/mL), respectively.

In 13 patients, ^{124}I -MIBG PET/CT was performed for known MMP. The mean patient age was 50.9 y (range, 17–80 y). Seven (54%) of these 13 patients were female, and 6 (46%) were male.

An overview of the MMP patient characteristics is provided in Table 2.

TABLE 1
Characteristics of Patients Who Underwent ^{124}I -MIBG PET for Suspected Pheochromocytoma

Characteristic	Data
Mean age (y)	51.8 (range, 20–74)
Sex (n)	
Male	18 (42%)
Female	25 (58%)
Catecholamine metabolites (pg/mL)	
Normetanephrines (plasma)	313.8 (28–2,358)
Metanephrines (plasma)	180.8 (15–1,377)
Mean size of adrenal mass (mm)	30 (range, 6–82)
Associated genetic syndrome (n)	
Multiple endocrine neoplasia IIA	3 (7%)
Neurofibromatosis	1 (2%)

^{124}I -MIBG Tumor Uptake

The mean SUV_{peak} across all lesions was 13.0, 13.3, 12.0, and 9.2 after 4 h, 1 d, 2 d, and 4 or 5 d, respectively. The tumor-to-background ratio at 4 h, 1 d, 2 d, and 4 or 5 d was 1.4, 6.2, 4.9, and 7.6, respectively. Because of the highest tumor SUV_{peak} and the highest number of available data points 1 d after ^{124}I -MIBG

TABLE 2
Characteristics of Patients Who Underwent ^{124}I -MIBG PET for Known Metastatic MMP

Characteristic	Data
Mean age (y)	50.9 (range, 17–81)
Sex (n)	
Male	6 (46%)
Female	7 (54%)
Tumor sites per patient (n)	
Adrenal gland	3 (23%)
Regional lymph nodes	5 (38%)
Bones	6 (46%)
Visceral, including distant lymph nodes	6 (46%)

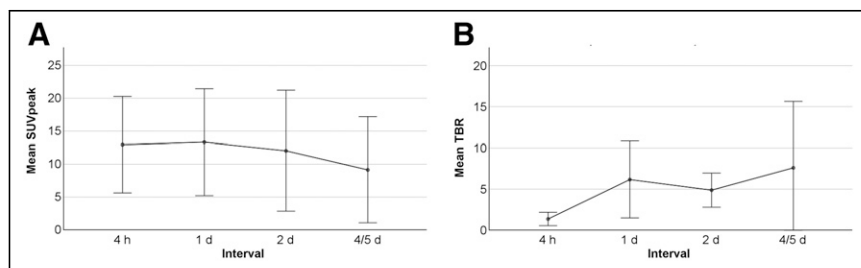


FIGURE 1. Simple error bar with 95% CI plotting mean tumor SUV_{peak} (A) and tumor SUV_{peak} /tumor SUV_{mean} (B) for all measured lesions in ^{124}I -MIBG PET-positive MMP patients ($n = 11$) over time.

injection, this time point was used for the subsequent accuracy analyses. In 3 patients, for whom ^{124}I -MIBG PET/CT was not performed 1 d after injection, 2-d images were used instead. Figure 1 shows the mean SUV_{peak} across all measured lesions and the mean tumor-to-background ratio over time.

^{124}I -MIBG PET Accuracy for Suspected Pheochromocytoma

^{124}I -MIBG PET was positive in 19 (44%) of 43 patients with suspected pheochromocytoma and negative in 24 (56%). In 1 of the 19 patients with positive findings on ^{124}I -MIBG PET, a local lymph node metastasis was detected. Twenty-five of the 43 patients had adrenal masses with a density of more than 10 HU on NC CT; in 22 of these, the respective masses were more than 10 mm.

The suspicion of pheochromocytoma was confirmed by the reference standard in 22 (51%) of the 43 patients and ruled out in 21 (49%). Histopathology was available in all cases with confirmed pheochromocytoma and in 3 (14%) of 21 cases in which the presence of pheochromocytoma was ruled out. Of the 22 patients with pheochromocytoma, 21 (95%) had unilateral involvement and 1 (5%) had bilateral involvement. In 18 (42%) of the 43 patients, the presence of pheochromocytoma was excluded on the basis of clinical records and repeated assessment of serum and urine catecholamine metabolites.

An overview of the diagnostic performance of ^{124}I -MIBG PET is provided in Table 3. Imaging was positive in 19 of 22 patients with confirmed pheochromocytoma and negative in 21 of 21 patients in whom the presence of pheochromocytoma was ruled out, resulting in a sensitivity and specificity of 86% and 100%, respectively.

In all patients with positive findings on ^{124}I -MIBG PET, pheochromocytoma was histopathologically confirmed, whereas 3 patients with a negative ^{124}I -MIBG PET result would later be diagnosed with pheochromocytoma, leading to a positive predictive value and negative predictive value of 100% and 88%, respectively.

NC CT was available for 36 patients. Of the 25 patients with adrenal masses greater than 10 HU, pheochromocytoma was confirmed in 18 and ruled out in 7; of the 11 patients with adrenal masses less than 10 HU, pheochromocytoma was confirmed in 1 and ruled out in 10, leading to a sensitivity, specificity, positive predictive value, and negative predictive value of 95%, 59%, 72%, and 91%, respectively.

Using an additional size threshold of 10 mm did not affect sensitivity but improved specificity, positive predictive value, and negative predictive value to 76%, 82%, and 93%, respectively.

Combined ^{124}I -MIBG PET and NC CT criteria improved the sensitivity to 100%, specificity to 76%, negative predictive value to 100%, and positive predictive value to 84%.

Pheochromocytomas had a significantly higher SUV_{peak} than did unaffected adrenal glands (11.8 vs. 3.5, $P < 0.001$). The area under the curve for the SUV_{peak} -based identification of pheochromocytoma was 0.88, with the optimal cutoff being 5.4. Subgroup analysis of all patients with adrenal lesions having a density higher than 10 HU showed an area under the curve of 0.90 (sensitivity, 68%; specificity, 100%) for classification into pheochromocytoma versus nonpheochromocytoma. Separate subgroup analyses of all patients with an

TABLE 3
Diagnostic Performance of ¹²⁴I-MIBG PET, NC CT, and Combined ¹²⁴I-MIBG PET and NC CT in Patients

Modality	Tumor present		Tumor absent		Diagnostic metrics				
	Scan+	Scan–	Scan+	Scan–	Sen	Spe	PPV	NPV	Acc
¹²⁴ I-MIBG PET	19	3	0	21	86%	100%	100%	88%	93%
¹²⁴ I-MIBG PET (NC CT available)	17	2	0	17	89%	100%	100%	89%	94%
HU > 10	18	7	1	10	95%	59%	72%	91%	78%
HU > 10; size > 10 mm	18	4	1	13	95%	76%	82%	93%	86%
¹²⁴ I-MIBG PET + NC CT	21	0	4	13	100%	76%	83%	100%	89%

Sen = sensitivity; Spe = specificity; Acc = accuracy.

indeterminate adrenal mass (HU > 10 and size > 10 mm; *n* = 22) showed an SUV_{peak} of 8.5 versus 2.9 (*P* < 0.001), resulting in an area under the curve of 0.90 (sensitivity, 72%; specificity, 100%) with an optimal cutoff of 7.0. Figure 2 gives an overview of the SUV_{peak} of patients for whom pheochromocytoma was confirmed versus those for whom it was ruled out.

¹²⁴I-MIBG PET Detection Rate for Metastatic Pheochromocytoma

In the 13 patients with known MMP lesions, increased focal ¹²⁴I-MIBG uptake was observed in 11 (85%). Combined CE CT and ¹²⁴I-MIBG PET detected 173 lesions, of which 166 (96%) showed increased ¹²⁴I-MIBG uptake, whereas 118 lesions (67%) were detected on standalone CE CT. This led to upstaging from M1a to M1c disease in 1 patient (8%) and migration from oligometastatic disease (>5 tumor sites) (26) in 3 (23%).

In 5 of these patients, additional ⁶⁸Ga-DOTATOC PET/CT was performed. ⁶⁸Ga-DOTATOC-positive/¹²⁴I-MIBG PET-negative lesions were found in 2 patients, and ⁶⁸Ga-DOTATOC-negative/¹²⁴I-MIBG PET-positive lesions were found in 1 patient. In the remainder, ⁶⁸Ga-DOTATOC PET and ¹²⁴I-MIBG PET yielded identical results with regard to lesion detection, but tumor-specific uptake was higher on ¹²⁴I-MIBG PET. Figure 3 shows an example MMP patient with positive ¹²⁴I-MIBG PET/CT results.

DISCUSSION

The present study reports high ¹²⁴I-MIBG PET accuracy at initial staging and a high detection rate at restaging in the—so far, to

our knowledge—largest published cohort of patients with (suspected) pheochromocytoma.

Image acquisition 1 d after ¹²⁴I-MIBG PET demonstrated the highest SUV_{peak}, and subsequent analyses were performed at this time point.

The reported sensitivity of the present study is comparable to that reported for ^{123/131}I-MIBG scintigraphy studies, and the specificity is close to the higher end of reported values (4,27–30). Sensitivity similar to that of ^{123/131}I-MIBG is unexpected, as the spatial resolution of PET imaging when compared with scintigraphy might translate into a higher accuracy. Interestingly, patients with false-negative ¹²⁴I-MIBG PET results did not have particularly small pheochromocytomas (3.0, 2.2, and 4.0 cm) when compared with the mean size of all resected pheochromocytomas (3.5 cm), implying that biology and norepinephrine transporter expression, rather than spatial resolution, are critical for lesion detection.

In line with the published literature, NC CT–based assessment has shown a high sensitivity, with only 1 false-negative finding, but at the expense of a low specificity.

Because ¹²⁴I-MIBG PET enables coacquisition of CE CT, NC CT, or MRI, the diagnostic performance might be improved over that of ¹²³I-MIBG scintigraphy, taking advantage of the high specificity of functional imaging and the high sensitivity of morphologic imaging. Therefore, complementary information from ¹²⁴I-MIBG PET might be of added value in the workup of unclear adrenal lesions when prior diagnostic imaging is inconclusive and to rule out or confirm metastatic spread before local treatment. In our cohort, visual interpretation of ¹²⁴I-MIBG images was superior to semiquantitative assessment for the diagnosis of pheochromocytoma. Further studies should assess the

potential diagnostic value of ¹²⁴I-MIBG kinetics in the diagnostic workup of adrenal lesions suggestive of pheochromocytoma. Because of an increase in tumor-to-background ratio over time, images acquired at late time points might aid the differentiation of tumor uptake from physiologic uptake in equivocal lesions.

¹²⁴I-MIBG PET/CT has also shown a high diagnostic performance in patients with MMP, demonstrating additional lesions compared with standalone CE CT in 7 (54%) of 13 patients, with TNM upstaging in 1 patient (8%) and stage migration from oligometastatic disease (26) to disseminated disease in

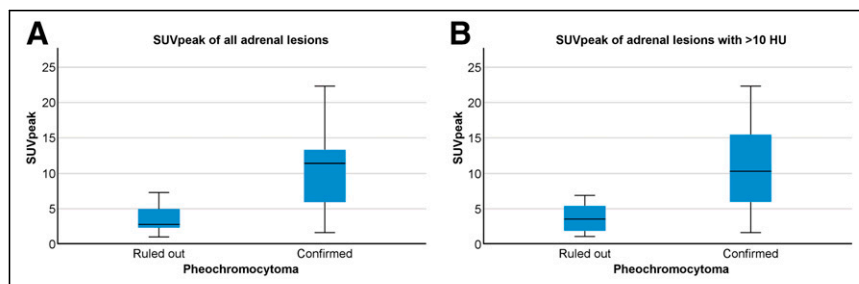


FIGURE 2. Adrenal SUV_{peak} for all patients (A) and patients with indeterminate adrenal masses (B) for whom pheochromocytoma was confirmed vs. those for whom it was ruled out.

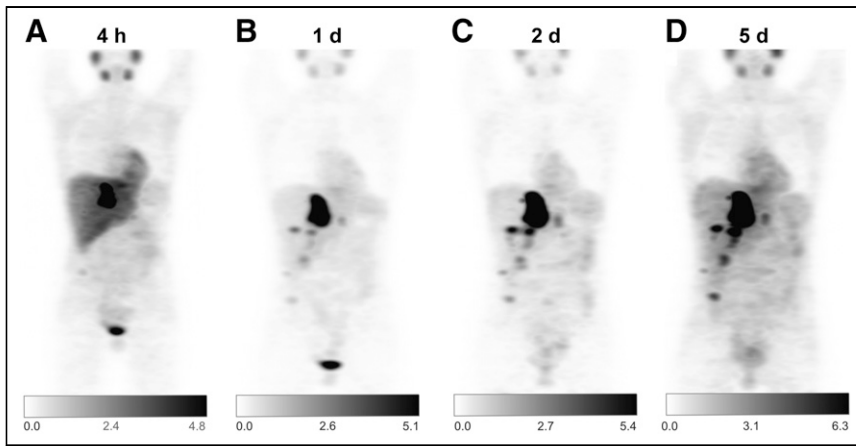


FIGURE 3. Example patient with metastatic MMP who underwent ^{124}I -MIBG PET/CT before planned radionuclide therapy. At 4 h (A), 1 d (B), 2 d (C), and 5 d (D) after image acquisition, dosimetry-derived activity of 20 GBq of ^{131}I -MIBG was administered, leading to lesion-absorbed doses of between 110 and 320 Gy and progression-free survival of 54 mo.

3 (23%). The high detection rate may impact patient staging, implementation of local treatment, and response assessment of systemic or local treatment. Detection of additional tumor sites might also prevent locoregional therapies in disseminated disease when little benefit is to be expected.

In light of the 2018 Food and Drug Administration approval of ^{131}I -MIBG radionuclide therapy for MIBG-positive unresectable, locally advanced or metastatic pheochromocytoma and paraganglioma, ^{124}I -MIBG PET/CT furthermore carries great potential for radionuclide therapy planning.

The long half-life or superior quantification of ^{124}I -MIBG PET/CT when compared with $^{123/131}\text{I}$ -MIBG scintigraphy facilitates an improved assessment of uptake intensity and kinetics (18,20,31–34). Pretherapeutic dosimetry of tumor lesions and organs at risk enables personalized dosimetry with the goal of maximizing tumor response while keeping toxicity levels acceptable. The potential of personalized dosimetry for ^{131}I therapy has previously been described in the context of differentiated thyroid cancer (25,35,36), but data on pheochromocytoma are scarce (18,34,37). In our cohort, 85% of patients with known MMP were MIBG-positive. In 2 patients with at least 1 ^{124}I -MIBG-negative lesion, intense ^{68}Ga -DOTATOC uptake was observed in all lesions, underpinning the theranostic potential of ^{68}Ga -/ ^{177}Lu -/ ^{90}Y -labeled somatostatin analogs (38). Prior small retrospective studies identified radiopeptide as a potential treatment option, leading to response rates of up to 50% and disease control rates of up to 100% (39–42).

Limitations of this study include the retrospective design and the small sample, as well as the absence of an adrenal-specific CT protocol and MR tomography.

CONCLUSION

^{124}I -MIBG PET detects pheochromocytoma with high accuracy at the initial work-up of adrenal masses and at restaging of metastatic disease. Accuracy was similar to that previously reported for $^{123/131}\text{I}$ -MIBG scintigraphy. Future studies on the impact of ^{124}I -MIBG PET on locoregional treatment and personalized ^{131}I -MIBG therapy, as well as a head-to-head comparison with $^{123/131}\text{I}$ -MIBG scintigraphy, are warranted.

DISCLOSURE

Manuel Weber reports fees from Boston Scientific (speakers bureau) outside the submitted work. Ken Herrmann reports personal fees from Bayer, SIRTEX, Adapcap, Curium, Endocyte, IPSEN, Siemens Healthineers, GE Healthcare, Amgen, Novartis, and ymabs; personal fees and other fees from Sofie Biosciences; non-financial support from ABX; and grants and personal fees from BTG outside the submitted work. Wolfgang P. Fendler reports fees from Calyx (consultant), RadioMedix (image review), Bayer (speakers bureau), and Parexel (image review) outside the submitted work. No other potential conflict of interest relevant to this article was reported.

KEY POINTS

QUESTION: What is the diagnostic performance of ^{124}I -MIBG PET in patients with known or suspected pheochromocytoma?

PERTINENT FINDINGS: ^{124}I -MIBG PET has a higher accuracy than NC CT in suspected pheochromocytoma and detects additional lesions in patients with known metastatic pheochromocytoma.

IMPLICATIONS FOR PATIENT CARE: ^{124}I -MIBG PET is a promising imaging technique that can provide information additional to that from cross-sectional imaging and thereby complement the diagnostic workup in patients with known or suspected pheochromocytoma.

REFERENCES

- Vallabhajosula S, Nikolopoulou A. Radioiodinated metaiodobenzylguanidine (MIBG): radiochemistry, biology, and pharmacology. *Semin Nucl Med.* 2011;41:324–333.
- Wiseman GA, Pacak K, O'Dorisio MS, et al. Usefulness of ^{123}I -MIBG scintigraphy in the evaluation of patients with known or suspected primary or metastatic pheochromocytoma or paraganglioma: results from a prospective multicenter trial. *J Nucl Med.* 2009;50:1448–1454.
- Bomanji J, Bouloux PM, Levison DA, et al. Observations on the function of normal adrenomedullary tissue in patients with pheochromocytomas and other paragangliomas. *Eur J Nucl Med.* 1987;13:86–89.
- Shapiro B, Copp JE, Sisson JC, Eyre PL, Wallis J, Beierwaltes WH. Iodine-131 metaiodobenzylguanidine for the locating of suspected pheochromocytoma: experience in 400 cases. *J Nucl Med.* 1985;26:576–585.
- Aboian MS, Huang SY, Hernandez-Pampaloni M, et al. ^{124}I -MIBG PET/CT to monitor metastatic disease in children with relapsed neuroblastoma. *J Nucl Med.* 2021;62:43–47.
- Vaz SC, Oliveira F, Herrmann K, Veit-Haibach P. Nuclear medicine and molecular imaging advances in the 21st century. *Br J Radiol.* 2020;93:20200095.
- Hofman MS, Kong G, Neels OC, Eu P, Hong E, Hicks RJ. High management impact of Ga-68 DOTATATE (GaTate) PET/CT for imaging neuroendocrine and other somatostatin expressing tumours. *J Med Imaging Radiat Oncol.* 2012;56:40–47.
- Hofman MS, Lawrentschuk N, Francis RJ, et al. Prostate-specific membrane antigen PET-CT in patients with high-risk prostate cancer before curative-intent surgery or radiotherapy (proPSMA): a prospective, randomised, multicentre study. *Lancet.* 2020;395:1208–1216.

9. Hofman MS, Emmett L, Sandhu S, et al. [¹⁷⁷Lu]Lu-PSMA-617 versus cabazitaxel in patients with metastatic castration-resistant prostate cancer (TheraP): a randomised, open-label, phase 2 trial. *Lancet*. 2021;397:797–804.
10. Kroiss A, Putzer D, Frech A, et al. A retrospective comparison between ⁶⁸Ga-DOTA-TOC PET/CT and ¹⁸F-DOPA PET/CT in patients with extra-adrenal paraganglioma. *Eur J Nucl Med Mol Imaging*. 2013;40:1800–1808.
11. Kroiss A, Putzer D, Decristoforo C, et al. ⁶⁸Ga-DOTA-TOC uptake in neuroendocrine tumour and healthy tissue: differentiation of physiological uptake and pathological processes in PET/CT. *Eur J Nucl Med Mol Imaging*. 2013;40:514–523.
12. Kroiss AS, Uprimny C, Shulkin BL, et al. ⁶⁸Ga-DOTATOC PET/CT in the localization of metastatic extra-adrenal paraganglioma and pheochromocytoma compared with ¹⁸F-DOPA PET/CT. *Rev Esp Med Nucl Imagen Mol*. 2019;38:94–99.
13. Kessler L, Schlitter AM, Kronke M, et al. First experience using ¹⁸F-flutrobenzguane PET imaging in patients with suspected pheochromocytoma or paraganglioma. *J Nucl Med*. 2021;62:479–485.
14. Lewington V, Lambert B, Poetschger U, et al. ¹²³I-MIBG scintigraphy in neuroblastoma: development of a SIOPEN semi-quantitative reporting, method by an international panel. *Eur J Nucl Med Mol Imaging*. 2017;44:234–241.
15. Ady N, Zucker JM, Asselain B, et al. A new ¹²³I-MIBG whole body scan scoring method: application to the prediction of the response of metastases to induction chemotherapy in stage IV neuroblastoma. *Eur J Cancer*. 1995;31A:256–261.
16. Beijst C, de Keizer B, Lam M, Janssens GO, Tytgat GAM, de Jong H. A phantom study: should ¹²⁴I-MIBG PET/CT replace ¹²³I-MIBG SPECT/CT? *Med Phys*. 2017;44:1624–1631.
17. Hicks RJ, Hofman MS. Is there still a role for SPECT-CT in oncology in the PET-CT era? *Nat Rev Clin Oncol*. 2012;9:712–720.
18. Huang SY, Bolch WE, Lee C, et al. Patient-specific dosimetry using pretherapy [¹²⁴I]m-iodobenzylguanidine ([¹²⁴I]mIBG) dynamic PET/CT imaging before [¹³¹I]mIBG targeted radionuclide therapy for neuroblastoma. *Mol Imaging Biol*. 2015;17:284–294.
19. Beijst C, Kist JW, Elschot M, et al. Quantitative comparison of ¹²⁴I PET/CT and ¹³¹I SPECT/CT detectability. *J Nucl Med*. 2016;57:103–108.
20. Jentzen W, Bockisch A, Ruhlmann M. Assessment of simplified blood dose protocols for the estimation of the maximum tolerable activity in thyroid cancer patients undergoing radioiodine therapy using ¹²⁴I. *J Nucl Med*. 2015;56:832–838.
21. Pettinato C, Monari F, Nanni C, et al. Usefulness of ¹²⁴I PET/CT imaging to predict absorbed doses in patients affected by metastatic thyroid cancer and treated with ¹³¹I. *Q J Nucl Med Mol Imaging*. 2012;56:509–514.
22. Plyku D, Hobbs RF, Huang K, et al. Recombinant human thyroid-stimulating hormone versus thyroid hormone withdrawal in ¹²⁴I PET/CT-based dosimetry for ¹³¹I therapy of metastatic differentiated thyroid cancer. *J Nucl Med*. 2017;58:1146–1154.
23. Ruhlmann M, Sonnenschein W, Nagarajah J, Binse I, Herrmann K, Jentzen W. Pretherapeutic ¹²⁴I dosimetry reliably predicts intratherapeutic blood kinetics of ¹³¹I in patients with differentiated thyroid carcinoma receiving high therapeutic activities. *Nucl Med Commun*. 2018;39:457–464.
24. Pryma DA, Chin BB, Noto RB, et al. Efficacy and safety of high-specific-activity ¹³¹I-MIBG therapy in patients with advanced pheochromocytoma or paraganglioma. *J Nucl Med*. 2019;60:623–630.
25. Klubo-Gwiezdzinska J, Van Nostrand D, Atkins F, et al. Efficacy of dosimetric versus empiric prescribed activity of ¹³¹I for therapy of differentiated thyroid cancer. *J Clin Endocrinol Metab*. 2011;96:3217–3225.
26. Hellman S, Weichselbaum RR. Oligometastases. *J Clin Oncol*. 1995;13:8–10.
27. Furuta N, Kiyota H, Yoshigoe F, Hasegawa N, Ohishi Y. Diagnosis of pheochromocytoma using [¹²³I]-compared with [¹³¹I]-metaiodobenzylguanidine scintigraphy. *Int J Urol*. 1999;6:119–124.
28. Rufini V, Troncone L, Valentini AL, Danza FM. A comparison of scintigraphy with radioiodinated MIBG and CT in localizing pheochromocytomas [in Italian]. *Radiol Med (Torino)*. 1988;76:466–470.
29. Mozley PD, Kim CK, Mohsin J, Jatlow A, Gosfield E III, Alavi A. The efficacy of iodine-123-MIBG as a screening test for pheochromocytoma. *J Nucl Med*. 1994;35:1138–1144.
30. Van Der Horst-Schrivers AN, Jager PL, Boezen HM, Schouten JP, Kema IP, Links TP. Iodine-123 metaiodobenzylguanidine scintigraphy in localising pheochromocytomas: experience and meta-analysis. *Anticancer Res*. 2006;26:1599–1604.
31. Kolbert KS, Pentlow KS, Pearson JR, et al. Prediction of absorbed dose to normal organs in thyroid cancer patients treated with ¹³¹I by use of ¹²⁴I PET and 3-dimensional internal dosimetry software. *J Nucl Med*. 2007;48:143–149.
32. Sgouros G, Hobbs RF, Atkins FB, Van Nostrand D, Ladenson PW, Wahl RL. Three-dimensional radiobiological dosimetry (3D-RD) with ¹²⁴I PET for ¹³¹I therapy of thyroid cancer. *Eur J Nucl Med Mol Imaging*. 2011;38(suppl 1):S41–S47.
33. Jentzen W, Freudenberg L, Eising EG, Sonnenschein W, Knust J, Bockisch A. Optimized ¹²⁴I PET dosimetry protocol for radioiodine therapy of differentiated thyroid cancer. *J Nucl Med*. 2008;49:1017–1023.
34. Seo Y, Gustafson WC, Dannoon SF, et al. Tumor dosimetry using [¹²⁴I]m-iodobenzylguanidine microPET/CT for [¹³¹I]m-iodobenzylguanidine treatment of neuroblastoma in a murine xenograft model. *Mol Imaging Biol*. 2012;14:735–742.
35. Hartung-Knemeyer V, Nagarajah J, Jentzen W, et al. Pre-therapeutic blood dosimetry in patients with differentiated thyroid carcinoma using ¹²⁴I-iodine: predicted blood doses correlate with changes in blood cell counts after radioiodine therapy and depend on modes of TSH stimulation and number of preceding radioiodine therapies. *Ann Nucl Med*. 2012;26:723–729.
36. Weber M, Binse I, Nagarajah J, Bockisch A, Herrmann K, Jentzen W. The role of ¹²⁴I PET/CT lesion dosimetry in differentiated thyroid cancer. *Q J Nucl Med Mol Imaging*. 2019;63:235–252.
37. Lee CL, Wahnische H, Sayre GA, et al. Radiation dose estimation using preclinical imaging with ¹²⁴I-metaiodobenzylguanidine (MIBG) PET. *Med Phys*. 2010;37:4861–4867.
38. Han S, Suh CH, Woo S, Kim YJ, Lee JJ. Performance of ⁶⁸Ga-DOTA-conjugated somatostatin receptor-targeting peptide PET in detection of pheochromocytoma and paraganglioma: a systematic review and metaanalysis. *J Nucl Med*. 2019;60:369–376.
39. Puranik AD, Kulkarni HR, Singh A, Baum RP. Peptide receptor radionuclide therapy with ⁹⁰Y/¹⁷⁷Lu-labelled peptides for inoperable head and neck paragangliomas (glomus tumours). *Eur J Nucl Med Mol Imaging*. 2015;42:1223–1230.
40. Zovato S, Kumanova A, Dematte S, et al. Peptide receptor radionuclide therapy (PRRT) with ¹⁷⁷Lu-DOTATATE in individuals with neck or mediastinal paraganglioma (PGL). *Horm Metab Res*. 2012;44:411–414.
41. Kong G, Grozinsky-Glasberg S, Hofman MS, et al. Efficacy of peptide receptor radionuclide therapy for functional metastatic paraganglioma and pheochromocytoma. *J Clin Endocrinol Metab*. 2017;102:3278–3287.
42. Forrer F, Riedweg I, Maecke HR, Mueller-Brand J. Radiolabeled DOTATOC in patients with advanced paraganglioma and pheochromocytoma. *Q J Nucl Med Mol Imaging*. 2008;52:334–340.